

# AERODYNAMIC OPTIMIZATION OF COAXIAL ROTOR IN HOVER AND AXIAL FLIGHT

**Omri Rand , Vladimir Khromov**  
**Faculty of Aerospace Engineering**  
**Technion, Israel Institute of Technology**  
**Haifa, 32000, Israel**

**Keywords:** *coaxial rotor, blade-element momentum theory, optimization, calculus of variation*

## Abstract

The paper presents an aerodynamic optimization of a coaxial rotor system in hover and axial flight. For that purpose, a suitable theorem of calculus of variations that provides a new generic result is employed. The analysis is founded on the Blade Element-Momentum Theory, which is based on nonlinear aerodynamics and mutual (interactional) influences that are introduced by the induced downwash field of each rotor over the other. The influence of non-uniformity of the downwash distribution on the optimal design was also studied. The analysis supplies an important insight into the optimal design and efficiency of coaxial rotor systems. The formulation is consistently generic and enables the exploration of a wide range of coaxial configurations.

## Nomenclature

<p><math>A</math> Disc square = <math>\pi R^2</math>.</p> <p><math>c_d</math> Drag coefficient.</p> <p><math>c_l</math> Lift coefficient.</p> <p><math>C_P</math> Power coefficient (= <math>P / (\rho A \Omega^3 R^3)</math>). All parameters belong to the rotor under discussion.</p> <p><math>C_T</math> Thrust coefficient (= <math>T / (\rho A \Omega^2 R^2)</math>). All parameters belong to the rotor under discussion.</p> <p><math>h</math> Rotor's clearance of the coaxial system.</p> <p><math>k</math> Influence coefficient.</p> <p><math>N_b</math> Number of blade.</p> <p><math>R</math> Disc radius.</p> <p><math>r</math> Spanwise location along the blade of the rotor</p>	<p>under discussion (<math>0 &lt; r &lt; R</math>).</p> <p><math>r_w</math> Upper rotor wake radius.</p> <p><math>T</math> Rotor thrust, positive upwards.</p> <p><math>V_t</math> Tip speed (= <math>\Omega R</math>).</p> <p><math>\alpha</math> Angle of attack.</p> <p><math>\gamma</math> Numerical coefficient in the expressions for <math>k</math>.</p> <p><math>\zeta_R</math> Coaxial system rotors radius ratio.</p> <p><math>\zeta_\Omega</math> Coaxial system angular velocities ratio.</p> <p><math>\eta</math> Lagrange multiplier.</p> <p><math>\theta_{pitch}</math> Blade pitch angle.</p> <p><math>\theta_{tw}</math> Blade twist angle.</p> <p><math>\kappa</math> Induced power correction coefficient.</p> <p><math>\lambda_C</math> Nondimensional climb velocity of the coaxial system (normalized by <math>\Omega^U R^U</math>).</p> <p><math>\lambda_C^{()}</math> Nondimensional "equivalent" climb velocity (normalized by <math>\Omega R</math> of the rotor under discussion).</p> <p><math>\lambda_i</math> Nondimensional induced velocity (normalized by <math>\Omega R</math> of the rotor under discussion).</p> <p><math>\rho</math> Air density.</p> <p><math>\Omega</math> Rotor angular velocity.</p> <p><math>()^U</math> Quantity related to the upper rotor.</p> <p><math>()^L</math> Quantity related to the lower rotor.</p> <p><math>()^{LI}</math> Quantity related to the inner part of the lower rotor.</p> <p><math>()^{LO}</math> Quantity related to the outer part of the lower rotor.</p> <p><math>\tilde{()}</math> Nondimensional length quantity, normalized by <math>R</math>.</p> <p><math>\bar{()}</math> Averaged quantity.</p> <p><math>()^*</math> Time averaged quantity.</p>
---	---

## INTRODUCTION

Different approaches to the aerodynamic analysis and optimization of coaxial helicopter rotors have been developed over the years, see e.g. Refs. [1], [2], [3], [4], [5]. A classical and well known result shows that in hover and axial flight, an optimal isolated rotor is a one with chord and twist that decrease as  $1/r$  where  $r$  is the spanwise location along the blade. Such a design provides a uniform inflow distribution and minimizes both the induced and the parasite power. Yet, similar analysis for a coaxial rotor system is much more involved and *the literature contains no explicit closed-form formulation for the problem of aerodynamically optimal coaxial system*. In most existing coaxial rotor analyses, the mutual influence between the two rotors is accounted for by prescribed downwash models.

## OPTIMIZATION METHODOLOGY

### Modeling and Fundamental Assumptions

The present paper deals with the optimal design of a coaxial rotor system in hover and axial climb. Fig. 1 shows a coaxial system of two concentric

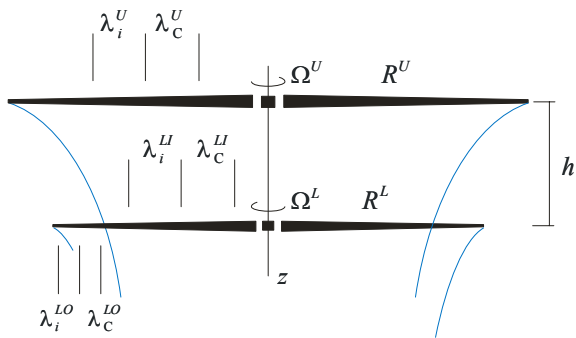


**Fig. 1** Coaxial rotor system in hover and climb.

rotors with a clearance,  $h$ , that rotate in opposite directions. The rotors are not necessarily identical in all parameters including their radius, rotational speed, number of blades, chord and airfoil

distribution, etc. (i.e.  $R^U \neq R^L$  and  $\Omega^U \neq \Omega^L$ ,  $N_b^U \neq N_b^L$ ,  $\tilde{c}^U(\tilde{r}) \neq \tilde{c}^L(\tilde{r})$  in the general case). We therefore define:

$$\zeta_R = \frac{R^L}{R^U}; \quad \zeta_\Omega = \frac{\Omega^U}{\Omega^L},$$

where for a constant tip speed we write  $\zeta_R = \zeta_\Omega = \zeta$ . We also define the spanwise location of the upper rotor's wake radius at the lower rotor plane (i.e. the wake contraction ratio or in other words the ratio of the upper rotor tip vortices radius at the lower rotor level over the upper rotor radius) as

$$\tilde{r}_w^U = \frac{R_w}{R^U}; \quad \tilde{r}_w^L = \frac{R_w}{R^L} = \frac{\tilde{r}_w^U}{\zeta_R}.$$

In this model, the upper rotor model takes into account the lower rotor induced velocity (in addition to the entire configuration climb velocity) as “equivalent climb speed” and similarly, the lower rotor model takes into account the upper rotor induced velocity as an “equivalent climb speed” as well. The present model is developed and presented in two parallel courses. The first course is founded on a simplified version of the above described interaction and therefore will be founded on mean (constant) influence coefficients. The second course will be focused on deriving a detailed description of the above described mutual influences.

The derivation of the above models was founded on the following sets of assumptions:

#### The simplified model:

a) It was assumed that the lower rotor downwash over the upper rotor disc area is uniform. Note that in some existing models it is even assumed to be small enough to be neglected, see e.g. Ref.[4].

b) The velocity induced by the upper rotor over the lower one is confined to a uniform downwash over its inner part (which is inside the

upper rotor's wake). The upper rotor's induced velocity over the outer part of the lower rotor is neglected.

The detailed model:

a) Experimental data and numerical free wake studies show that the downwash of the lower rotor over the upper rotor disc is not uniform, it has a relatively large value at the hub and it tends to diminish towards the disc perimeter. The effect of such non-uniformity will be demonstrated in what follows.

b) The upper rotor's induced velocity over the outer part of the lower rotor is usually of small magnitude.

c) Generic distribution of the upper rotor downwash over the lower inner rotor disc area will be studied. In some models it is assumed to be nonuniform and distributed along the radius as it is distributed over the upper rotor radius. Consequently, in hover, it is assumed that  $\lambda_C^{LI}(\tilde{r}^L) = k^{UL}\lambda_i^U(\tilde{r}^L/\tilde{r}_w^U)$  where  $0 < \tilde{r}^L < \tilde{r}_w^U$ .

Assumptions that will be applied to both models:

a) The effect of the interaction of the upper rotor's wake with the lower rotor's wake is neglected.

b) Sharp boundary between the region in the lower rotor that is inside the upper rotor wake and that which is outside it is assumed. Despite the sharp changes in the induced velocity and the effective angles of attack, two-dimensional analysis is assumed to remain valid in this transition area as well.

**The Mutual Interaction Between the Rotors**

As indicated above, the upper rotor is submerged in the downwash that is induced by the lower rotor. This downwash is written as  $k^{LU}\bar{\lambda}_i^L\frac{\zeta_R}{\zeta_\Omega}$  where  $k^{LU}$  is an influence coefficient and  $\bar{\lambda}_i^L$  is the av-

eraged nondimensional induced velocity over the lower rotor. In general,  $k^{LU}$  is a function of  $\tilde{r}^U$ , and therefore, a constant (mean) value of  $k^{LU}$  stands for uniform influence of the lower rotor on the upper one. Similarly, the inner part of the lower rotor (which is inside the upper rotor's wake) is submerged in the downwash that is induced by the upper rotor and is written as  $k^{UL}\bar{\lambda}_i^U\frac{\zeta_\Omega}{\zeta_R}$  where  $k^{UL}$  is an influence coefficient and  $\bar{\lambda}_i^U$  is the averaged nondimensional induced velocity over the upper rotor. Clearly,  $k^{UL}$  is a function of  $\tilde{r}^L$ . Hence in the general case, the equivalent climb velocities over the upper and the lower rotors are:

$$\lambda_C^U(\tilde{r}) = k^{LU}(\tilde{r})\bar{\lambda}_i^L\frac{\zeta_R}{\zeta_\Omega} + \lambda_C, \quad (1)$$

$$\lambda_C^L(\tilde{r}) = [k^{UL}(\tilde{r})\bar{\lambda}_i^U + \lambda_C]\frac{\zeta_\Omega}{\zeta_R}. \quad (2)$$

$\lambda_C$  is the climb velocity of the system (normalized by the tip speed of the upper rotor). Note that  $\bar{\lambda}_i^L$  and  $\bar{\lambda}_i^U$  are the averaged induced velocity over the *disc areas* and are therefore expressed as:

$$\bar{\lambda}_i^U = 2 \int_0^1 \tilde{r}\lambda_i^U(\tilde{r})d\tilde{r}; \quad \bar{\lambda}_i^L = 2 \int_0^1 \tilde{r}\lambda_i^L(\tilde{r})d\tilde{r}.$$

The simplified model: In the simplified model discussed above, we assume that  $k^{LU}$  is constant, and  $k^{UL}$  is constant for  $\tilde{r}^L < \tilde{r}_w^L$  and vanishes for  $\tilde{r}_w^L < \tilde{r}^L < 1$ . As will be proved later on, in such a case,  $\lambda_i^U(\tilde{r})$  of the optimal design turns to be also constant. Similarly,  $\lambda_i^L(\tilde{r})$  becomes constant for  $\tilde{r}^L < \tilde{r}_w^L$  (and will be denoted  $\lambda_i^{LI}$  there), while it takes a value of different constant for  $\tilde{r}_w^L < \tilde{r}^L < 1$  (and will be denoted  $\lambda_i^{LO}$  there). Hence, in such a case, the equivalent climb velocities are given by:

$$\lambda_C^U = \quad (3)$$

$$k^{LU} \left\{ (\tilde{r}_w^L)^2 \lambda_i^{LI} + [1 - (\tilde{r}_w^L)^2] \lambda_i^{LO} \right\} \frac{\zeta_R}{\zeta_\Omega} + \lambda_C,$$

and

$$\lambda_C^L = [k^{UL}\lambda_i^U + \lambda_C]\frac{\zeta_\Omega}{\zeta_R}, \quad (4)$$

$$\lambda_C^{LO} = \lambda_C \frac{\zeta_\Omega}{\zeta_R}. \quad (5)$$

### Estimation of the influence coefficients and wake contraction ratio in hover

The estimation of the influence coefficients  $k^{UL}(\tilde{r}^L)$  and  $k^{LU}(\tilde{r}^U)$  and the wake contraction ratio  $\tilde{r}_w^L$  will be discussed in what follows by two stages. For the simplified model, we shall first deal with the averaged values of  $k^{UL}(\tilde{r}^L)$  and  $k^{LU}(\tilde{r}^U)$  and  $\tilde{r}_w^L$  as functions of the rotors clearance  $\tilde{h} = h/R$ . Later on, a more detailed distributions of the above coefficients and a modified wake contraction function will be discussed for the detailed model.

The estimation of the averaged values is described in details in Ref.[3] with comparison to experimental data. Subsequently, the averaged induced velocity are given by

$$k^{UL} = 1 + \left( \frac{d}{\sqrt{1+d^2}} \right)^{\gamma_{UL}}; \quad k^{LU} = 1 - \left( \frac{d}{\sqrt{1+d^2}} \right)^{\gamma_{LU}}$$

where  $d = |h/R^U|$  for the upper rotor and  $d = |h/R^L|$  for the lower rotor,  $\gamma_{UL} = 0.6$  and  $\gamma_{LU} = 0.3 \div 0.5$  - see Fig. 2. Hence, momentum arguments show that the wake contraction is given by

$$\tilde{r}_w^U = \sqrt{\frac{1}{k^{UL}}}.$$

Fig. 3 presents a free wake geometry of a single rotor. The wake contraction is clearly observed. The induced velocity of such a wake is not uniform in the general case. The resulting influence coefficients in such a case are expressed as:

$$k^{UL}(\tilde{r}^L) = \frac{\lambda^{*L}(\tilde{r}^L)}{\bar{\lambda}_i^U \frac{\zeta_\Omega}{\zeta_R}}; \quad k^{LU}(\tilde{r}^U) = \frac{\lambda^{*U}(\tilde{r}^U)}{\bar{\lambda}_i^L \frac{\zeta_R}{\zeta_\Omega}}$$

where  $\lambda^{*U}(\tilde{r}^U)$  and  $\lambda^{*L}(\tilde{r}^L)$  are the time averaged values as functions of the radial stations.

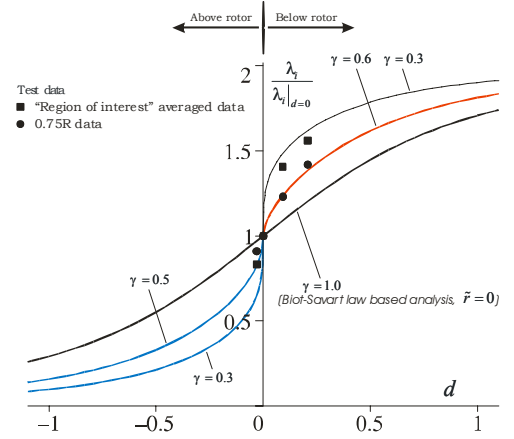


**Fig. 2** Averaged induced velocity distribution below and above a single rotor.

### The Proposed Optimal Coaxial System Analysis

The proposed analysis is based on a *calculus of variations theorem* that exploits the *Blade Element-Momentum Theory* with nonlinear aerodynamics including mutual rotor influences and rigorously solves the problem of aerodynamically optimal coaxial rotor.

For aerodynamically optimal rotor, two basic conditions should be fulfilled: (a) the induced velocity distribution should be the one that minimizes the induced power; (b) each cross-section should work in its optimal angle of attack to maximize its  $c_l/c_d$ . The optimization of the induced power results in the induced velocity distribution which thereafter, together with the parasite power minimization, leads to the optimal chord and twist distributions.

**Induced Power:** It is well known that constant induced velocity minimizes the induced power for a single rotor that is subjected to a uniform (along the blade span) external downwash. Assuming that  $k^{LU}$  is constant, or in other words, the “equivalent climb” of the upper rotor (due to the lower rotor) is uniform, the above condition of constant induced velocity may be applied. However, for the lower rotor, the external downwash induced by the upper rotor is not uniform

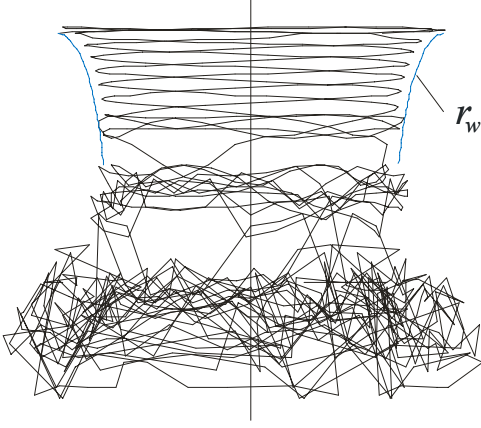


**Fig. 3** Free Wake Geometry in Hover.

and exhibit a large change between the region which is inside the upper rotor's wake and the part which is outside the upper rotor's wake. In other words,  $k^{UL}(\tilde{r}^L)$  is not constant (and as already discussed, the most simplified acceptable assumption may be  $k^{UL} = c_1$  for  $\tilde{r}^L < \tilde{r}_w^L$  and  $k^{UL} = c_2$  for  $\tilde{r}^L > \tilde{r}_w^L$ , where  $c_1$  and  $c_2$  are constants).

To rigorously obtain the optimal condition when  $k^{UL}$  is not constant, a new calculus of variations based optimal condition which is based on the *Blade Element-Momentum Theory* has been derived. To clarify and support the following discussion, it should be mentioned that the *Blade Element-Momentum Theory* determines the induced velocity by equating the thrust distribution per unit length as separately obtained by the “momentum” and the “blade element” theories, namely:

$$4\pi\rho r (V_C + v_i) v_i = \frac{1}{2} N_b \rho \Omega^2 r^2 c_l(\alpha),$$

where the effective angle of attack is given by

$$\alpha = \theta_{pitch} + \theta_{tw}(\tilde{r}) - \tan^{-1} \left( \frac{\lambda_C + \lambda_i}{\tilde{r}} \right).$$

In a nondimensional form we write the above as

$$8\pi(\lambda_C + \lambda_i)\lambda_i = N_b \tilde{r} \tilde{c} c_l(\alpha), \quad (6)$$

where in the general case, the nondimensional chord,  $\tilde{c}$ , and the nondimensional induced velocity,  $\lambda_i$ , are functions of  $\tilde{r}$ . In the coaxial analysis case, and as will be shown in what follows,  $\lambda_C$  should be considered as function of  $r$  as well. Note that  $c_l$  is also a function of  $r$  due to the nonuniform distribution of airfoils, the variation in the effective angle of attack,  $\alpha$ , and the dependency of the aerodynamic characteristics on Mach and Reynolds numbers.

Consequently, one may express the thrust and induced power coefficients as

$$C_T = 4 \int_0^1 \tilde{r} (\lambda_C + \lambda_i) \lambda_i d\tilde{r}, \quad (7)$$

$$C_{Pi} = 4 \int_0^1 \tilde{r} (\lambda_C + \lambda_i)^2 \lambda_i d\tilde{r}. \quad (8)$$

For a given climb velocity distribution,  $\lambda_C(\tilde{r})$ , the induced power optimization task is focused on the selection of  $\lambda_i(\tilde{r})$ , that for a given thrust coefficient,  $C_T$ , as given by Eq.(7), will minimize  $C_{Pi}$  as given by Eq.(8). For that purpose we employ the *calculus of variations technique* and adopt the minimization process of an integral of the form

$$J = \int_0^1 F(\tilde{r}, \lambda_i, \frac{d\lambda_i}{d\tilde{r}}) d\tilde{r},$$

while for the present case of optimization with constraint (minimum induced power for a given thrust) we define:

$$F = C_{Pi} + \eta C_T,$$

where  $\eta$  is a Lagrange multiplier. Hence,  $J$  takes the form:

$$J = \int_0^1 \left\{ 4\tilde{r}(\lambda_C + \lambda_i)^2 \lambda_i + \eta [4\tilde{r}(\lambda_C + \lambda_i) \lambda_i] \right\} d\tilde{r}.$$

The above integrand shows that  $\lambda_i(\tilde{r})$  should fulfill the following Euler equation

$$\frac{\partial F}{\partial \lambda_i} = \frac{\partial \left\{ \tilde{r}(\lambda_C + \lambda_i)^2 \lambda_i + \eta [\tilde{r}(\lambda_C + \lambda_i) \lambda_i] \right\}}{\partial \lambda_i} = 0$$

or

$$\tilde{r} (\lambda_C^2 + \eta \lambda_C + 4\lambda_C \lambda_i + 2\eta \lambda_i + 3\lambda_i^2) = 0. \quad (9)$$

**Parasite Power:** As far as the parasite power optimization is concerned, each blade cross-section should operate in its optimal effective angle of attack,  $\alpha_{opt}$ , where the ratio  $c_l/c_d$  is maximal, and, hence, we define  $c_l^{opt} = c_l(\alpha_{opt})$ ,  $c_d^{opt} = c_d(\alpha_{opt})$ .

## Blade Design, Thrust and Power

**Chord Distribution:** In the general case, Eq.(6) shows that

$$\tilde{c}^X(\tilde{r}) = \frac{8\pi [\lambda_C^X(\tilde{r}) + \lambda_i^X(\tilde{r})] \lambda_i^X(\tilde{r})}{N_b^X} \frac{1}{\tilde{r} c_l^{opt}(\tilde{r})}, \quad (10)$$

where  $0 < \tilde{r}^X < 1$  and  $X = L, U$ .

The simplified case: For the upper rotor where  $\lambda_C^U$  is constant, the above Euler equation (Eq.(9)) shows that  $\lambda_i^U$  should be constant as well. Thus, Eq.(6) shows that the chord distribution should take the form:

$$\tilde{c}^U(\tilde{r}) = \frac{8\pi (\lambda_C^U + \lambda_i^U) \lambda_i^U}{N_b^U} \frac{1}{\tilde{r} c_l^{opt}(\tilde{r})} \quad (11)$$

for  $0 < \tilde{r} < 1$ , while for the lower rotor, the above Euler equation shows that different constant values should be assigned to the inner and outer parts of the lower rotor, and therefore:

$$\tilde{c}^{LI}(\tilde{r}) = \frac{8\pi (\lambda_C^{LI} + \lambda_i^{LI}) \lambda_i^{LI}}{N_b^L} \frac{1}{\tilde{r} c_l^{opt}(\tilde{r})},$$

for ( $0 < \tilde{r} < \tilde{r}_w^L$ ) and

$$\tilde{c}^{LO}(\tilde{r}) = \frac{8\pi (\lambda_C^{LO} + \lambda_i^{LO}) \lambda_i^{LO}}{N_b^L} \frac{1}{\tilde{r} c_l^{opt}(\tilde{r})}$$

for ( $\tilde{r}_w^L < \tilde{r} < 1$ ). As will be shown in the examples presented in what follows, an introduction of relatively small cut-out removes the singularity at  $\tilde{r} = 0$  but practically does not damage the optimal efficiency.

**Twist Distribution:** To ensure that  $\alpha_{opt}^X(\tilde{r})$  matches the required distribution over the entire upper and lower blades (as dictated by the airfoil distribution and Mach and Reynolds number distributions) and by requiring  $(\theta_{tw}^X)_{\tilde{r}=\frac{3}{4}} = 0$ , the twist distribution and the pitch angle are given by:

$$\theta_{tw}^X(\tilde{r}) = \alpha_{opt}^X(\tilde{r}) - \theta_{pitch}^X + \tan^{-1} \left( \frac{\lambda_C^X(\tilde{r}) + \lambda_i^X(\tilde{r})}{\tilde{r}} \right),$$

$$\theta_{pitch}^X = (\alpha_{opt}^X)_{\tilde{r}=\frac{3}{4}} + \tan^{-1} \left( \frac{(\lambda_C^X)_{\tilde{r}=\frac{3}{4}} + (\lambda_i^X)_{\tilde{r}=\frac{3}{4}}}{3/4} \right)$$

where  $X = L, U$ .

The simplified case: for the upper

$$\theta_{tw}^U(\tilde{r}) = \alpha_{opt}^U(\tilde{r}) - \theta_{pitch}^U + \tan^{-1} \left( \frac{\lambda_C^U + \lambda_i^U}{\tilde{r}} \right),$$

$$\theta_{pitch}^U = (\alpha_{opt}^U)_{\tilde{r}=\frac{3}{4}} + \tan^{-1} \left( \frac{\lambda_C^U + \lambda_i^U}{3/4} \right).$$

Similarly, to ensure that  $\alpha_{opt}^L(\tilde{r})$  matches the required distribution over the entire lower blade and by requiring  $(\theta_{tw}^L)_{\tilde{r}=\frac{3}{4}} = 0$ , the twist distribution over the lower rotor and its pitch angle are given by:

$$\theta_{tw}^{LI}(\tilde{r}) = \alpha_{opt}^L(\tilde{r}) - \theta_{pitch}^L + \tan^{-1} \left( \frac{\lambda_C^{LI} + \lambda_i^{LI}}{\tilde{r}} \right),$$

$$\theta_{tw}^{LO}(\tilde{r}) = \alpha_{opt}^L(\tilde{r}) - \theta_{pitch}^L + \tan^{-1} \left( \frac{\lambda_C^{LO} + \lambda_i^{LO}}{\tilde{r}} \right),$$

$$\theta_{pitch}^L = (\alpha_{opt}^L)_{\tilde{r}=\frac{3}{4}} + \tan^{-1} \left( \frac{\lambda_C^{LY} + \lambda_i^{LY}}{3/4} \right),$$

where

$$\begin{cases} Y \Rightarrow I & \text{for } \tilde{r}_w^L > 3/4 \\ Y \Rightarrow O & \text{for } \tilde{r}_w^L < 3/4 \end{cases}.$$

As already indicated regarding the chord distribution, in the actual design the twist does not reach infinite value at  $\tilde{r} = 0$ .

**Thrust:** In the general case Eq.(7) should be employed.

The simplified case: Since  $\lambda_i^U$  and  $\lambda_C^U$  are constants, the thrust of the upper rotor is given by, see Eq.(7),

$$C_T^U = 2(\lambda_C^U + \lambda_i^U) \lambda_i^U. \quad (12)$$

Similarly since  $\lambda_i^{LI}$ ,  $\lambda_i^{LO}$ ,  $\lambda_C^{LI}$  and  $\lambda_C^{LO}$  are constants, for the lower rotor we define

$$C_T^L = C_T^{LI} + C_T^{LO},$$

where

$$C_T^{LI} = 2(\lambda_C^{LI} + \lambda_i^{LI}) \lambda_i^{LI} \cdot (\tilde{r}_w^L)^2,$$

$$C_T^{LO} = 2(\lambda_C^{LO} + \lambda_i^{LO}) \lambda_i^{LO} [1 - (\tilde{r}_w^L)^2].$$

**Induced Power:** In the general case Eq.(8) should be employed.

The simplified case: Using Eq.(8), the power coefficients for the upper rotor is defined as

$$C_{Pi}^U = 2(\lambda_C^U + \lambda_i^U)^2 \lambda_i^U,$$

and therefore by employing Eq.(12)

$$C_{Pi}^U = (\lambda_C^U + \lambda_i^U) C_T^U. \quad (13)$$

Similarly, for the lower rotor:

$$C_{Pi}^L = (\lambda_C^L + \lambda_i^L) C_T^L + (\lambda_C^{LO} + \lambda_i^{LO}) C_T^{LO}.$$

**Parasite Power:** The parasite power

$$P_d = N_b \Omega \int_0^R \frac{1}{2} \rho \Omega^2 r^2 c r c_d^{opt} dr,$$

may be written in its nondimensional form as:

$$C_{Pd}^X = \frac{N_b^X}{2\pi} \int_0^1 \tilde{r}^3 \tilde{c}^X(\tilde{r}) c_d^{opt}(\tilde{r}) d\tilde{r},$$

where  $X = U, L$ .

The simplified case: In the simplified case, using Eqs.(7,11,12)

$$C_{Pd}^U = 2C_T^U \int_0^1 \frac{c_d^{opt}(\tilde{r})}{c_l^{opt}(\tilde{r})} \tilde{r}^2 d\tilde{r}, \quad (14)$$

which for a uniform blade becomes

$$C_{Pd}^U = \frac{2}{3} C_T^U \frac{c_d^{opt}}{c_l^{opt}}. \quad (15)$$

Similarly for the lower rotor as:

$$C_{Pd}^L = \frac{2C_T^{LI}}{(\tilde{r}_w^L)^2} \int_0^{\tilde{r}_w^L} \frac{c_d^{opt}(\tilde{r})}{c_l^{opt}(\tilde{r})} \tilde{r}^2 d\tilde{r} +$$

$$\frac{2C_T^{LO}}{1 - (\tilde{r}_w^L)^2} \int_{\tilde{r}_w^L}^1 \frac{c_d^{opt}(\tilde{r})}{c_l^{opt}(\tilde{r})} \tilde{r}^2 d\tilde{r}.$$

### The downwash distribution effect

Figure 4 shows various downwash distributions along the blade while the average downwash velocity is the same for all cases. The table in this

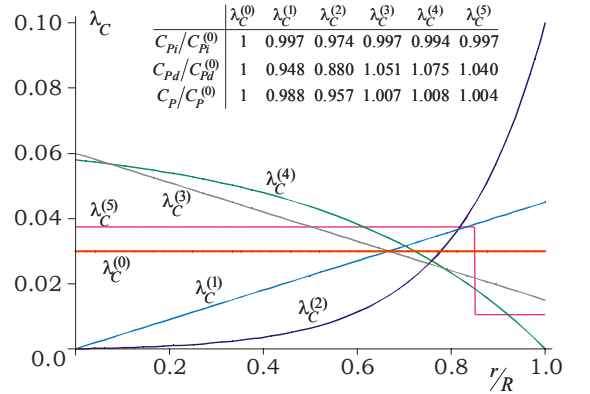


**Fig. 4** Various downwash distributions along the blade with a comparison of the required power.

figure shows the induced and parasite power required for the same thrust value. Note that for each downwash distribution - a different optimal rotor design is required.

Figure 5 shows the effective angle attack for various downwash distributions along the blade when the blades were design for uniform (average) downwash velocity distribution. The resulting power values in this case are clearly higher than those shown in Fig. 4.

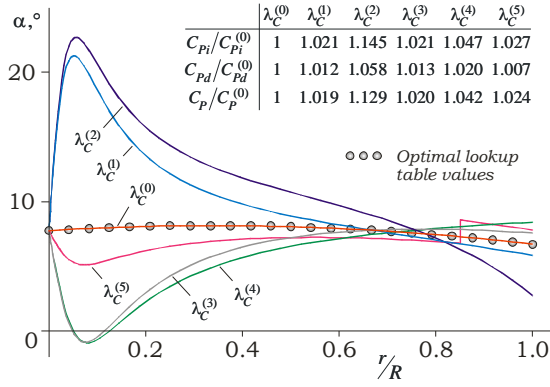


**Fig. 5** Effective angle of attack for various downwash distributions.

## THE SOLUTION SCHEME

In the general case, the above described optimization of a coaxial rotor system is expressed as a nonlinear system of 4 equations and unknowns, namely:

$$f_i(x_1 \dots x_4) \quad \text{for } i = 1 \dots 4$$

where the unknowns are  $x_1 = \bar{\lambda}_i^U$  and  $x_2 = \bar{\lambda}_i^L$  and  $x_3 = \eta^U$   $x_4 = \eta^L$ . For a given set of these four values, the following calculations should be executed:

- Calculate  $\lambda_C^U(\bar{r})$  and  $\lambda_C^L(\bar{r})$  by Eqs.(1,2).
- Calculate  $\lambda_i^U(\bar{r})$  and  $\lambda_i^L(\bar{r})$  from Eq.(9) as:

$$\lambda_i^X(\bar{r}) = \frac{1}{3} \left( -A_\lambda + \sqrt{B_\lambda} \right)$$

where

$$A_\lambda = 2\lambda_C^X(\bar{r}) + \eta^X$$

$$B_\lambda = (\lambda_C^X(\bar{r}))^2 + \eta^X \lambda_C^X(\bar{r}) + (\eta^X)^2$$

and  $X = U, L$ .

- Calculate the residual functions:

$$f_1 = C_T - C_T^{TOTAL}$$

$$f_2 = C_{Pi}^U + C_{Pd}^U - [C_{Pi}^L + C_{Pd}^L] \frac{\zeta_R^5}{\zeta_\Omega^2}$$

$$f_3 = \bar{\lambda}_i^U - 2 \int_0^1 \bar{r} \lambda_i^U(\bar{r}) d\bar{r}$$

$$f_4 = \bar{\lambda}_i^L - 2 \int_0^1 \bar{r} \lambda_i^L(\bar{r}) d\bar{r}$$

Thus, by employing a nonlinear solver, the values of  $x_i$  that yield  $f_i = 0$  are found.

### The simplified case:

In the simplified case, the above optimization problem may be expressed as the following nonlinear algebraic system of 9 equations and unknowns:

$$\begin{aligned} (\lambda_C^U)^2 + \eta^U \lambda_C^U + 4\lambda_C^U \lambda_i^U + 2\eta^U \lambda_i^U + 3(\lambda_i^U)^2 &= 0, \\ (\lambda_C^{LI})^2 + \eta^L \lambda_C^{LI} + 4\lambda_C^{LI} \lambda_i^{LI} + 2\eta^L \lambda_i^{LI} + 3(\lambda_i^{LI})^2 &= 0, \\ (\lambda_C^{LO})^2 + \eta^L \lambda_C^{LO} + 4\lambda_C^{LO} \lambda_i^{LO} + 2\eta^L \lambda_i^{LO} + 3(\lambda_i^{LO})^2 &= 0, \\ \lambda_C^U &= k^{LU} \left\{ (\bar{r}_w^L)^2 \lambda_i^{LI} + [1 - (\bar{r}_w^L)^2] \lambda_i^{LO} \right\} \frac{\zeta_R}{\zeta_\Omega} + \lambda_C, \\ \lambda_C^{LI} &= [k^{UL} \lambda_i^U + \lambda_C] \frac{\zeta_\Omega}{\zeta_R}, \\ C_T^U &= 2(\lambda_C^U + \lambda_i^U) \lambda_i^U, \\ C_T^L &= C_T^{LI} + C_T^{LO}, \\ C_T^{TOTAL} &= C_T^U + C_T^L \frac{\zeta_R^4}{\zeta_\Omega^2}, \\ C_{Pi}^U + C_{Pd}^U &= [C_{Pi}^L + C_{Pd}^L] \frac{\zeta_R^5}{\zeta_\Omega^2}, \end{aligned} \quad (16)$$

where the unknowns are

$$C_T^U, C_T^L, \lambda_C^U, \lambda_C^{LI}, \lambda_C^{LO}, \lambda_i^U, \lambda_i^{LI}, \lambda_i^{LO}, \eta^U, \eta^L,$$

and

$$\lambda_C^{LO} = \lambda_C \frac{\zeta_\Omega}{\zeta_R}.$$

Note that  $C_T^{TOTAL}$  represents the total required trust and that the last equation of Eqs.(16) stands for the torque balance condition which is required in a coaxial system.

### Illustrative Limiting Cases

At this stage it is worth mentioning few limiting cases:

- For very closed rotors (zero clearance,  $h/R = 0$ ) two identical rotor are first discussed.

Each rotor produces the same thrust ( $C_T/2$ ) and induced velocity ( $\lambda_i$ ) and is submerged in the other rotor's downwash which should be considered as "equivalent climb". Hence, in this case,  $k^{UL} = k^{LU} = 1$  and  $\tilde{r}_w^U = 1$  and the induced velocity for a rotor in climb is

$$\lambda_i = -\frac{\lambda_C}{2} + \sqrt{\frac{\lambda_C^2}{4} + \frac{C_T/2}{2}}$$

Substituting  $\lambda_C = \lambda_i$  yields:

$$\lambda_i = \frac{1}{2} \sqrt{\frac{C_T}{2}}$$

Hence the total inflow,  $2\lambda_i = \sqrt{\frac{C_T}{2}}$ , is identical to the one produced by a single rotor of  $C_T$ . The induced and parasite power components become (see Eqs.(13,15)),

$$C_{Pi} = 2 \times (\lambda_i + \lambda_C) \frac{C_T}{2} = \sqrt{\frac{C_T^3}{2}}$$

$$C_{Pd} = 2 \times \frac{2}{3} \frac{C_T}{2} \frac{c_d^{opt}}{c_l^{opt}}. \quad (17)$$

which is exactly the value created by a single rotor of  $C_T$ .

b) For tandem configuration, where two identical rotors, each produce thrust of  $C_T/2$  and  $k^{UL} = k^{LU} = 0$

$$\lambda_i = \sqrt{\frac{C_T/2}{2}},$$

and hence,

$$C_{Pi} = 2 \times \lambda_i \frac{C_T}{2} = \frac{1}{\sqrt{2}} \sqrt{\frac{C_T^3}{2}}$$

and  $C_{Pd}$  is identical to the one shown in Eq.(17).

### Rotor Efficiency

Two different quantities may be used for the examination of rotor efficiency. The first one

is the rotor's Figure of Merit (FM) that is defined as the **ratio of the ideal induced power** ( $P_i = \sqrt{T^3/(2\rho A)}$ ) **over the total power**. In all cases discussed,  $T$  stands for the total system's thrust and  $A$  stands for the total disc areas in the system. Yet, as will be shown later on, a much more important parameter is the (dimensional) power loading defined by the **ratio of the thrust over the power**.

**Single non-optimal rotor:** For a (non-optimal) rotor of constant chord one may write

$$T = \frac{N_b}{6} \rho \Omega^2 c \bar{c}_l R^3; \quad P_D = \frac{N_b}{8} \rho \Omega^3 c \bar{c}_d R^4,$$

where  $\bar{c}_l$  and  $\bar{c}_d$  are the averaged drag and lift coefficients given by

$$\bar{c}_l = \frac{3}{R^3} \int_0^R r^2 c_l dr; \quad \bar{c}_d = \frac{4}{R^4} \int_0^R r^3 c_d dr.$$

Hence,  $P_D = T^{\frac{3}{4}} V_t \frac{\bar{c}_d}{\bar{c}_l}$  where  $V_t = \Omega R$ , and

$$FM = \frac{\sqrt{\frac{T}{A}}}{\kappa \sqrt{\frac{T}{A}} + \frac{3}{4} \sqrt{2\rho} V_t \frac{\bar{c}_d}{\bar{c}_l}}.$$

$\kappa$  is a correction that applies to the actual induced power in a non-optimal rotor. It mainly accounts for the inflow nonuniformity:

$$\kappa = \frac{1}{\sqrt{2}} \frac{\int_0^1 \tilde{r} \lambda_i^3(\tilde{r}) d\tilde{r}}{\left[ \int_0^1 \tilde{r} \lambda_i^2(\tilde{r}) d\tilde{r} \right]^{3/2}}.$$

Substituting a linear variation of  $\lambda_i$  in the above yields a value of  $\kappa \simeq 1.13$ , which is close to typical measured values.

The ratio of the thrust over the power is then given by

$$\frac{T}{P} = \frac{FM}{\sqrt{\frac{T}{2\rho A}}} = \frac{\sqrt{2\rho}}{\kappa \sqrt{\frac{T}{A}} + \frac{3}{4} \sqrt{2\rho} V_t \frac{\bar{c}_d}{\bar{c}_l}}.$$

**Single optimal rotor:** Based on Eqs.(13,14), one may write for a single optimal rotor

$$FM = \frac{\lambda_i}{\lambda_i + 2 \int_0^1 \frac{c_d^{opt}(\tilde{r})}{c_l^{opt}(\tilde{r})} \tilde{r}^2 d\tilde{r}},$$

where  $\lambda_i = \sqrt{\frac{C_T}{2}}$ . By noting that  $\frac{T}{A} = C_T \rho V_t^2$ , we write

$$FM = \frac{\sqrt{\frac{T}{A}}}{\sqrt{\frac{T}{A} + 2V_t \sqrt{2\rho} \int_0^1 \frac{c_d^{opt}(\tilde{r})}{c_l^{opt}(\tilde{r})} \tilde{r}^2 d\tilde{r}}},$$

which yields (note that  $\kappa = 1$  in this case)

$$\frac{T}{P} = \frac{FM}{\sqrt{\frac{T}{2\rho A}}} = \frac{\sqrt{2\rho}}{\sqrt{\frac{T}{A} + 2V_t \sqrt{2\rho} \int_0^1 \frac{c_d^{opt}(\tilde{r})}{c_l^{opt}(\tilde{r})} \tilde{r}^2 d\tilde{r}}}.$$

**Coaxial system:** assuming constant tip speed,  $V_t$  (where  $\zeta_R = \zeta_\Omega = \zeta$ ), we write the “ $T/A$ ” and “ $T/P$ ” quantities as

$$\begin{aligned} \frac{T^U + T^L}{A^U + A^L} &= \frac{1}{1 + \zeta^2} (C_T^U + C_T^L \zeta^2) \rho V_t^2, \\ \frac{T^U + T^L}{P^U + P^L} &= \frac{C_T^U + C_T^L \zeta^2}{C_P^U + C_P^L \zeta^2} \frac{1}{V_t}. \end{aligned}$$

which yields

$$\begin{aligned} FM &= \sqrt{\frac{1}{2\rho} \frac{T}{P}} \sqrt{\frac{T}{A}} \\ &= \sqrt{\frac{1}{2(1 + \zeta^2)} \frac{(C_T^U + C_T^L \zeta^2)^2}{C_P^U + C_P^L \zeta^2}}. \end{aligned}$$

For identical rotors ( $\zeta = 1$ ), this value may be interpreted as the *ratio between the ideal induced power required by a single (isolated) rotor of area  $2A$  (or, since tip speed is assumed constant, two (isolated) rotors each of area  $A$ ) to the actual required power in a coaxial system.*

## TYPICAL RESULTS

Figure 6 presents power loading vs. disc loading for a non-optimal rotor, optimal rotor and a coaxial optimal system. In this figure,  $\rho = 1.2 \text{ Kg/m}^3$ ,  $V_t = 180 \text{ m/s}$ ,  $c_d^{opt}/c_l^{opt} = \bar{c}_d/\bar{c}_l \simeq 1/40$  (a typical value of NACA0012) and  $h/R = 0.2$ .

It is first shown that  $FM$  is increasing with  $T/A$  for all configuration while  $T/P$  is decreasing. Hence  $FM$  is certainly not a comprehensive enough criterion for efficiency. Three working

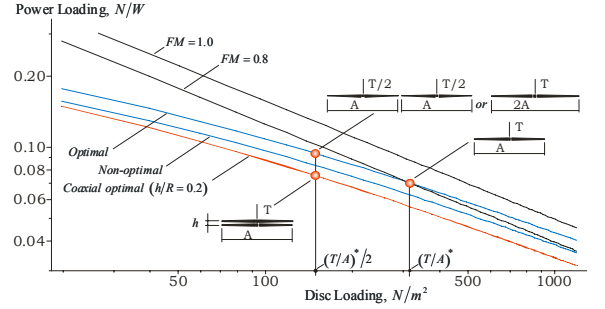


**Fig. 6** Power loading vs. Disc loading for non-optimal rotor, optimal rotor and a coaxial system.

point are shown in Fig. 6: a single rotor with a typical disc loading,  $(T/A)^*$ , a tandem configuration with an extra identical rotor (and therefore with a half of the disc loading) and a coaxial optimal system with the same disc loading  $(T/2A)^*$ . Clearly, moving from a single to a tandem configuration yields a much higher  $T/P$  ratio due to the decreasing disc loading. The contribution of this paper at this particular context is in the rigorous evaluation of the interference effects that reduce this  $T/P$  ratio to a lower level as shown for a coaxial system in Fig. 6.

Fig. 7 presents the variation of the optimal angle of attack in a typical NACA0012 airfoil as function of the radial station. This variation is mainly due to the Mach number variation along the blade. As shown, the exact data that is obtained from the (discrete) tables is piecewise-constant and is not continuous due to the employed lookup table technique. It is therefore smoothed and fed into the analysis.

Figs. 8 presents the variation of  $c_l$  vs. angle of attack and Mach number for the NACA0012 airfoil. The red cross-curves show the optimal values that maximize its  $c_l/c_d$ .

Fig. 9 presents the torque coefficient of a single optimal rotor compared with a variety of typical rotors of constant chord (in the range of 5 - 8% of the radius) and linear twist (in the range

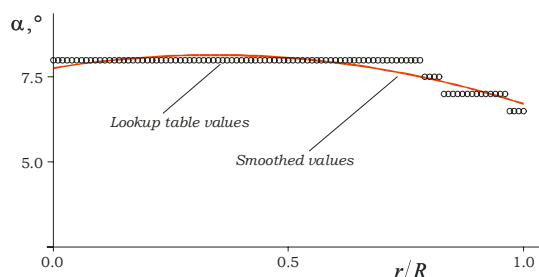


**Fig. 7** Optimal angle of attack variation as function of the radial station.

of  $5^\circ - 30^\circ$ ). In all optimal rotor calculations, the (optimal) twist and chord distributions were not changed while cut-out was introduced. As shown, optimal conditions may not be achieved with constant chord and linear twist. Note that in this example, for a cut-out that is larger than 0.3, the optimal values lose their applicability.

Similar comparison for a coaxial configurations is presented in Fig. 10. As expected, optimal conditions may not be achieved with constant chord and linear twist in this case as well.

Fig. 11 presents a comparison of the induced velocity distribution in optimal and non optimal coaxial configuration. As shown, in the optimal case (with and without cut-out), the induced velocity is uniform for the upper rotor and piecewise uniformly distributed for the lower rotor. In the case of constant chord and linear twist, the induced velocity is a function of the radial station.

Typical chord and twist distributions for optimal coaxial rotor are present in Fig. 12,13.

Finally, Fig. 14 presents two typical single and coaxial optimal rotor designs.

## CONCLUSION

An aerodynamics optimization methodology for a coaxial rotor system in hover and axial flight that is based on clear and basic physical reason-

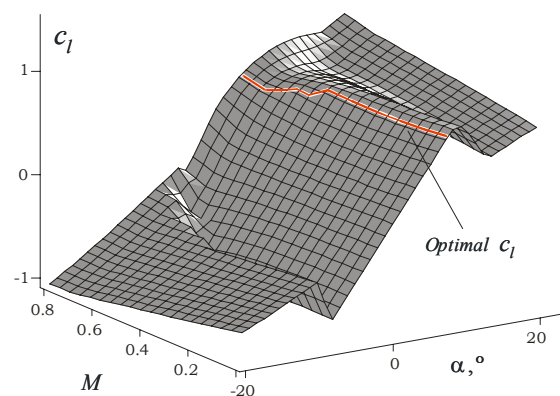


**Fig. 8** Lift coefficient of the example airfoil data.

ing, is offered. The optimization study is evaluated by suitable *theorem of calculus of variations* and provides a new generic result. The methodology is based on introducing the interactional inflow fields into the *Blade Element-Momentum Theory* while using real nonlinear aerodynamic tables.

## REFERENCES

- [1] Nagashima T. and Nakanishi K. Optimum performance and wake geometry of a co-axial rotor in hover. *Vertica*, 7(3):225–239, 1983.
- [2] Bourtsev B.N., Kvokov V.N., Vainstein I.M., and Petrosian E.A. Phenomenon of a coaxial helicopter high figure of merit at hover. In *23rd European Rotorcraft Forum*, Germany, 1997.
- [3] McAlister K.W., Tung C., Rand O., Khromov V., and Wilson J.S. Experimental and numerical study of a model coaxial rotor. In *Additional Proceedings Papers of the American Helicopter Society 62nd Annual Forum*, Phoenix, Arizona, 2006.
- [4] Leishman J.G. and Ananthan S. An optimum coaxial rotor system for axial flight. *Journal of the American Helicopter Society*, 53(4):366–381, 2008.
- [5] Juhasz O., Syal M., Celi R., Khromov V., Rand O., Ruzicka G.C., and Strawn R.C. A comparison of three coaxial aerodynamic prediction methods including validation with model test data. In *Pro-*

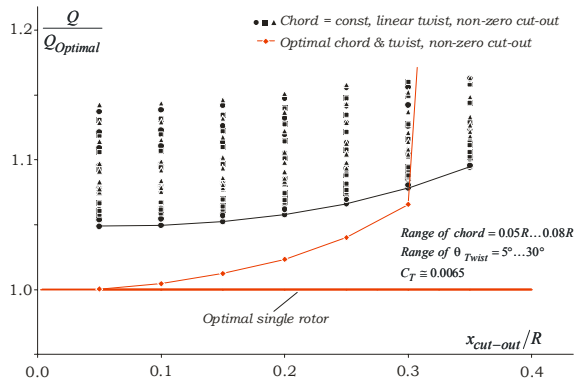


**Fig. 9** Torque coefficient of a single optimal and non-optimal rotors.

*ceedings Papers of the 2010 AHS Aeromechanics Specialists' Conference, San Francisco, CA, 2010.*

**Copyright Statement**

The authors confirm that they, and/or their company or organization, hold copyright on all of the original material included in this paper. The authors also confirm that they have obtained permission, from the copyright holder of any third party material included in this paper, to publish it as part of their paper. The authors confirm that they give permission, or have obtained permission from the copyright holder of this paper, for the publication and distribution of this paper as part of the ICAS2010 proceedings or as individual off-prints from the proceedings.

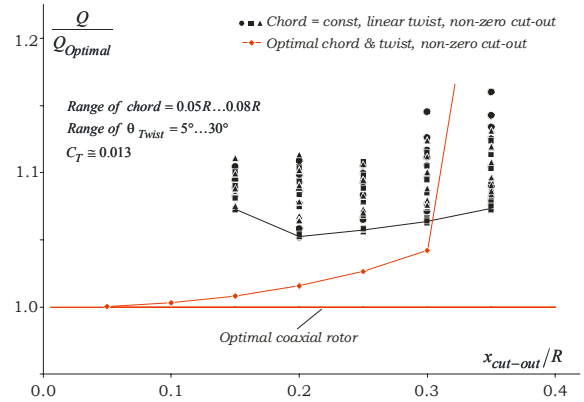


**Fig. 10** Torque coefficient of a coaxial optimal and non-optimal rotors.

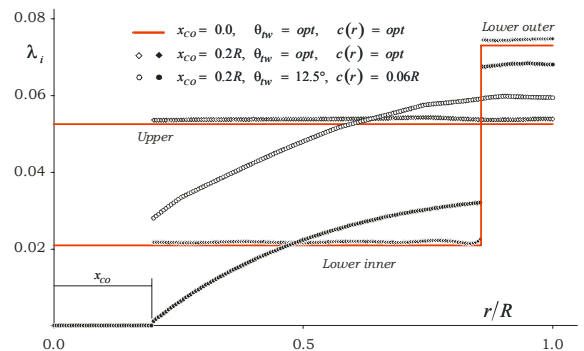


**Fig. 11** Comparison of the induced velocity distribution in optimal and non optimal configuration.

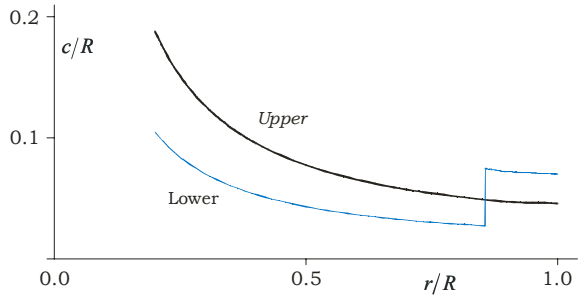


**Fig. 12** Coaxial optimal rotor chord distribution.

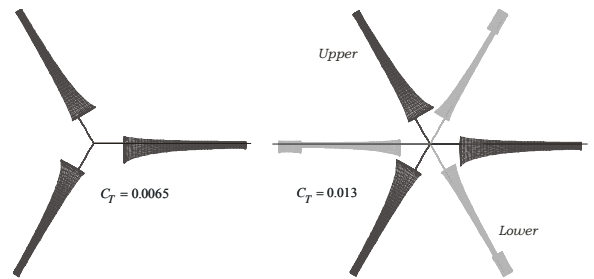


**Fig. 14** Two typical single and coaxial optimal rotor chord distributions (top view, no twist).

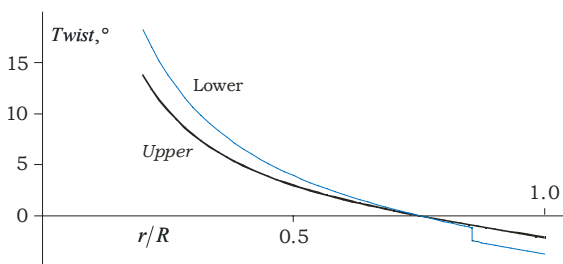


**Fig. 13** Coaxial optimal rotor twist distribution.